Study of Differences between Sunspot and White Light Facular Area Data Determined from SDO/HMI and SOHO/MDI Observations

L. Győri

Abstract Sunspot and white light facular areas are important data of solar activity and are used, for example, in the study of the evolution of sunspots and their effect on solar irradiance. *Solar Dynamic Observatory's Helioseismic and Magnetic Imager* (SDO/HMI) solar images have much higher resolution ($\sim 0.5''\text{pixel}^{-1}$) than *Solar and Heliospheric Observatory's Michelson Doppler Imager* (SOHO/MDI) solar images ($\sim 2''\text{pixel}^{-1}$). This difference in image resolution has a significant impact on the sunspot and white light facular areas measured in the two datasets. We compare the area of sunspots and white light faculae derived from SDO/HMI and SOHO/MDI observations. This comparison helps the calibration of the SOHO sunspot and facular area to those in SDO observations. We also find a 0.22 degree difference between the north direction in SDO/HMI and SOHO/MDI images.

Keywords: Sunspots, Areas; White Light Faculae, Areas

1. Introduction

There are two types of motivation for this work: practical and principal. The observable solar features, such as white light faculae and sunspots, are one manifestation of energy transfer processes in the Sun. One of the most important parameters of sunspots and white light faculae is their area, which is used directly or as proxies in many fields of investigation. Precise area measurements are especially important for the study of solar irradiance (Fröhlich et al, 1994; Fligge and Solanki, 1997) and for solar cycle studies (Oliver and Ballester, 1994; Chapman et al, 2011). Of course, the measured values of feature areas depend on the methods used to find them and the image quality and characteristics (Baranyi et al., 2001; Wenzler et al., 2004). Therefore, it is of practical importance to compare the feature areas obtained from *Solar and Heliospheric Observatory's Michelson Doppler Imager* (SOHO/MDI; Scherrer et al., 1995) and *Solar Dynamic Observatory's Helioseismic and Magnetic Imager* (SDO/HMI; Scherrer et

Debrecen Heliophysical Observatory, Gyula Observing
Station, P.O. Box 93, 5701 Gyula, Hungary
email: gylajos@tigris.unideb.hu

al., 2012; Pesnell et al., 2012) observations so as to have a more reliable longer time series of space-based sunspot area data.

Another practical reason is that we, at the Debrecen Observatory, compiled two SOHO/MDI based catalogues (sunspots and white-light faculae) and continue to compile two similar SDO/HMI based catalogues. Thus, it is useful to adjust SOHO/MDI and SDO/HMI catalogues to each other.

The principal reason for this study is to find out how the resolution of the solar images influences the measured area of the solar features. For this purpose the two datasets provided by the SOHO (Domingo, Fleck, and Poland, 1995) and the SDO satellites are well suited because there is no seeing effect as in the case of ground based observation, and because, due to their high-cadence of observation, it is easier to find nearly co-temporal observations in order to exclude differences caused by the development of the features.

2. Observations

In this paper we compare two full-disk solar image series: SOHO/MDI (1024 x 1024 pixels), and SDO/HMI (4096 x 4096 pixels).

They are obtained as proxies for the continuum intensity. MDI observes the full solar disk in the Ni I absorption line at 676.8 nm, and HMI in the Fe I absorption line at 617.3 nm.

For the comparison purpose 2200 image pairs, each taken within 2 minutes, and covering the time interval (from 1 May 2010 to 11 April 2011) of the common operation of the two satellites, were chosen.

There are many erroneous pixels and pixel groups in the MDI images in the years of 2010 and 2011. They may bias the feature area measurements, therefore the MDI images are first preprocessed. The erroneous pixels are found and patched by using the average intensity value of their environment.

3. Effect of Image Resolution on Solar Feature Area

Differences in solar feature areas between image sets with different resolutions can be attributed to three causes:

- *Border inaccuracy.* One pixel inaccuracy around the border of a solar feature has more influence on the feature area in images with lower resolution. For example, in the case of the HMI and the MDI images, one MDI border pixel represents 16 times more area on the solar disk than one HMI pixel. The overall effect of the border inaccuracy on the area depends very much on the raggedness of the border. Generally, the *border inaccuracy* effect makes the feature area larger for lower resolution images (Győri et al., 2004)).
- *Structural adequacy.* How well the real structure of a solar feature is mirrored in a solar image depends on the resolution of the image. For example, long thin fissures inside a solar feature do not show up in a lower resolution
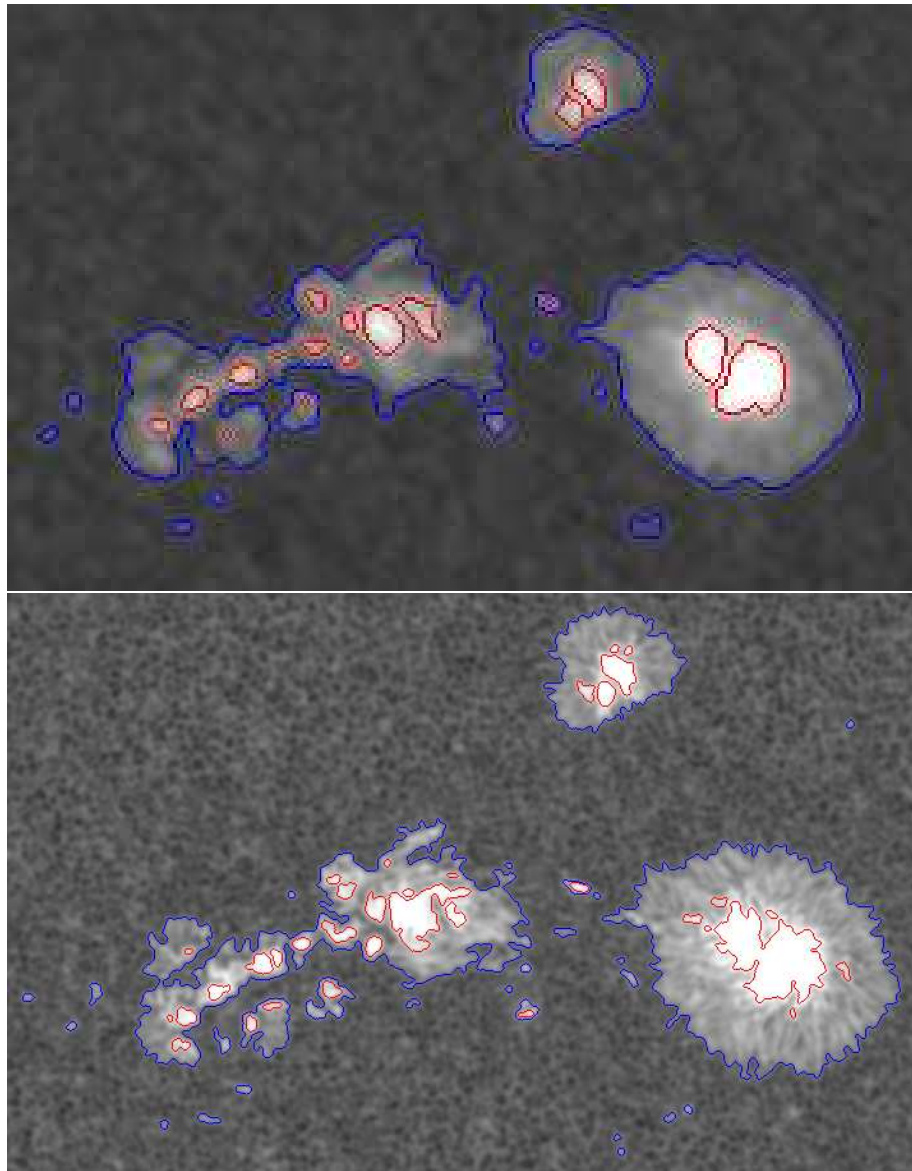
Figure 1. The same sunspot area (NOAA AR 11117) in MDI (top; 27 October 2010 00:01:31 UT) and HMI (bottom; 27 October 2010 00:00:30.50 UT) inverse images. Blue and red colors represent penumbra and umbra borders, respectively.

image, and so its area is included into the area of the feature. Similarly, nearby, standalone features separated by narrow gaps merge in a lower resolution image. The *structural adequacy* effect also makes the feature area larger for lower resolution images.

- *Feature perceivability.* Features that are small (below or around one pixel) and less intensive dissolve into their environment, and so they can not
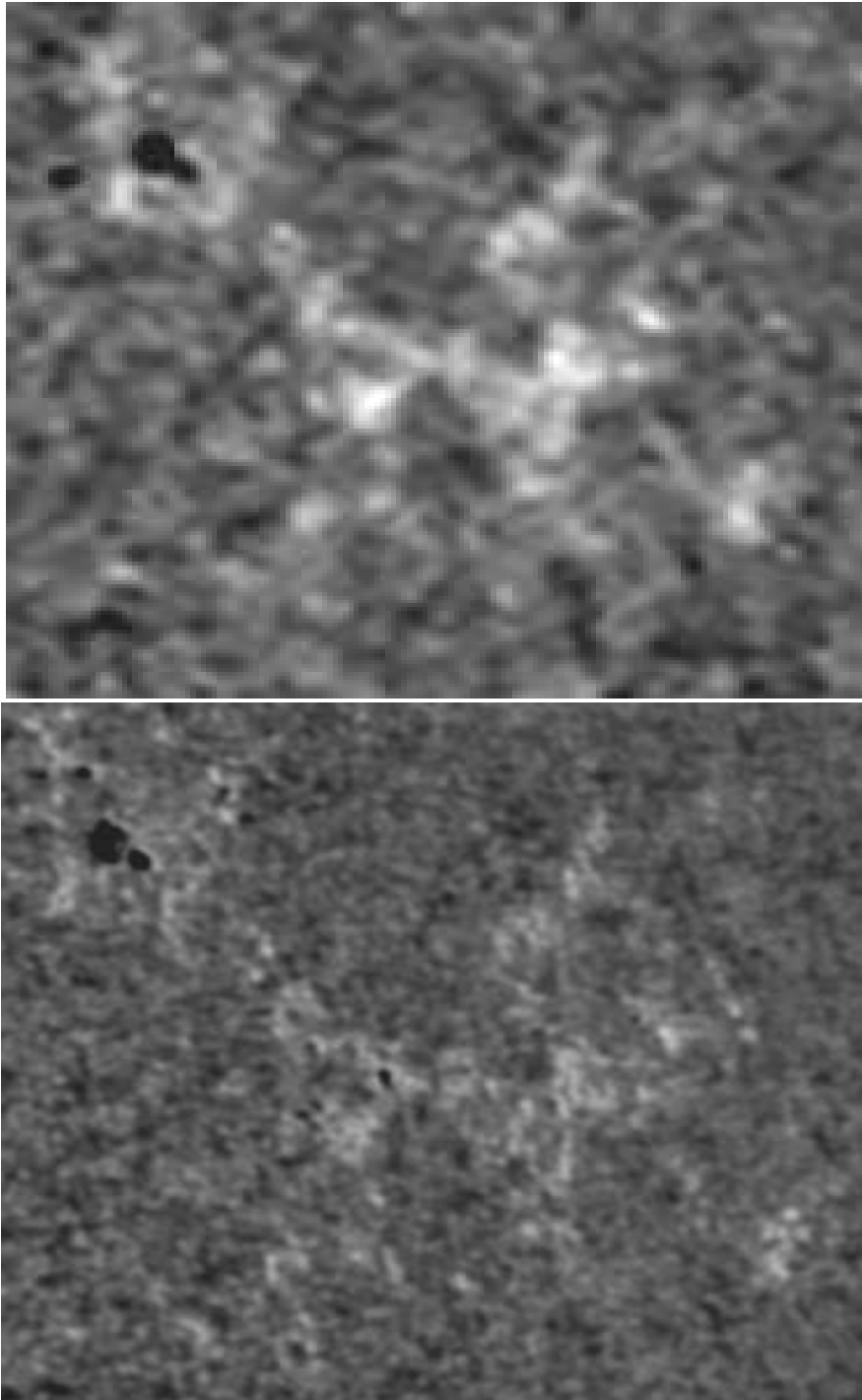
Figure 2. The same facular area in MDI (top) and HMI (bottom) images. The two images were taken within one minute.

be perceived. The *feature perceivability* effect makes the total feature area smaller for lower resolution images.

Figure 1 and Figure 2 provide examples of these effects. Figure 1 shows the same sunspot group in the MDI (upper panel) and in the HMI (lower panel) images. The two images were taken about within one minute. Blue and red lines represet the penumbra and umbra borders of the spots. Owing to the better resolution of the HMI images, even in smaller sunspots, the umbra separates away from the penumbra background, and also in large penumbrae, even the small umbrae separate from the penumbra background. Thus they can be perceived as observed in the HMI image, while they do not show up in the MDI image. In the HMI image, we can also observe several small sunspots (pores) that can not be seen in the MDI image.

Figure 2 shows the same facular area in the MDI (upper panel) and in the HMI (lower panel) images. The two images were taken within 1 minute. The typical size of the solar facular grains is below $1''$ (e.g., Bovelet and Wiehr, 2001) while the image scale of the MDI images is $\sim 2'' pixel^{-1}$. Therefore an extension induced by the low resolution, of the facular area appears. This effect can be well seen in Figure 2. As can seen the nearby, individual facluar grains in the HMI image merge into one large facular area in the MDI image.

4. Methods

4.1. Finding Sunspot and Faculae

To determine sunspot and white light facular areas, the software package SAM (Sunspot Automatic Measurement) (Győri, 1998) was used. Actually, SAM is a set of computer programs. These programs cooperate in order to embrace every aspect of compiling solar feature catalogues (sunspots and white-light faculae).

First, SAM preprocesses the solar image. The preprocessing can be broken down two main parts: determining the solar disk parameters (the solar disk radius, the positions of the disk center, and the image direction relative to heliographic North) that are needed to transform image coordinates into heliographic ones, and several kinds of correction that may depend on how the solar image was obtained (CCD camera, photographic plate, ground-based, space-borne), and what is known about the telescope that acquired it (optical distortion, image tilt).

A few more words about one of the solar disk parameters, namely about the image direction, because this parameter will cause some problems when we automatically identify, *i.e.* find the corresponding, sunspots in HMI and MDI images. SAM can get the image direction relative to the heliographic North in several ways: it can determine it from the image itself, if the images contain some kind of direction markers (Győri, 2005), it can be provided as an input parameter or file, or it can be read out from the image file header, if it is included. In the case of the HMI and MDI images the direction of solar north is read from the FITS header of the image.

Having preprocessed the image, SAM decomposes it into an ordered (with respect to the containment relation) contour set in such a way that, at different intensity levels (the cadence is derived from the standard deviation of the undisturbed photoshere), all the iso-density contours are determined. Combining this contour set with the gradient image (edge map), SAM is able to explore the fine structures of the solar features, and, among others, determine their positions and areas.

An example of the sunspot (umbra and penumbra) boundaries determined by SAM can be seen in Figure 1.

4.2. Comparing Areas

The relationship between solar features areas (sunspot and white light facula) in the two imageries is modeled by linear regression. We can, in principle, choose to treat either of the two areas as the independent variable. But we have a practical reason to choose the MDI area as independent variable. This reason is that we think that the HMI measured areas are more accurate than MDI ones, therefore we want to transform MDI areas into HMI ones, and to this end, we need the MDI areas as independent variable.

Using the parameters obtained by the linear regression fit we can transform MDI areas into HMI ones and with this we can introduce the Transformed Relative Area Difference ($TRAD$) defined as

$(HMI\ area\ -\ transformed\ MDI\ area)/transformed\ MDI\ area.$

To give a visual impression on how accurately the linear regression model reproduces the HMI areas from the MDI ones, beside the figure showing the scatter plot and the regression line fitted to the feature areas in the two imageries, an additional figure is provided. This figure depicts TRAD *vs.* transformed MDI areas.

For a visual demonstration of the results, the projected areas are used, but the parameters of the linear regression fit to the areas corrected for foreshortening are also given.

Projected areas are measured in millionths of the solar disk (md) and corrected areas in millionths of the solar hemisphere (mh).

For the sake of clarity, we define some terms used in the paper. Sunspot area is the area of the whole spot (umbra + penumbra) or the area of a pore (a small sunspot without penumbra, lighter than an umbra). Total sunspot area is the area of the sunspots summed up on the whole solar disk. Umbra area is the area of the umbra of the sunspot, pores are excluded. Total sunspot umbra area is the area of the umbrae summed up on the whole solar disk.

4.3. Identifying Sunspots

If we compare the areas of the same spots measured in the HMI and the MDI images we can get rid of the *structural adequacy* (partly) and the *feature perceivability* effects of the image resolution and so we can investigate how the resolution influences the accuracy of finding the spot borders. To this end, we must find the corresponding sunspots in HMI and MDI images.
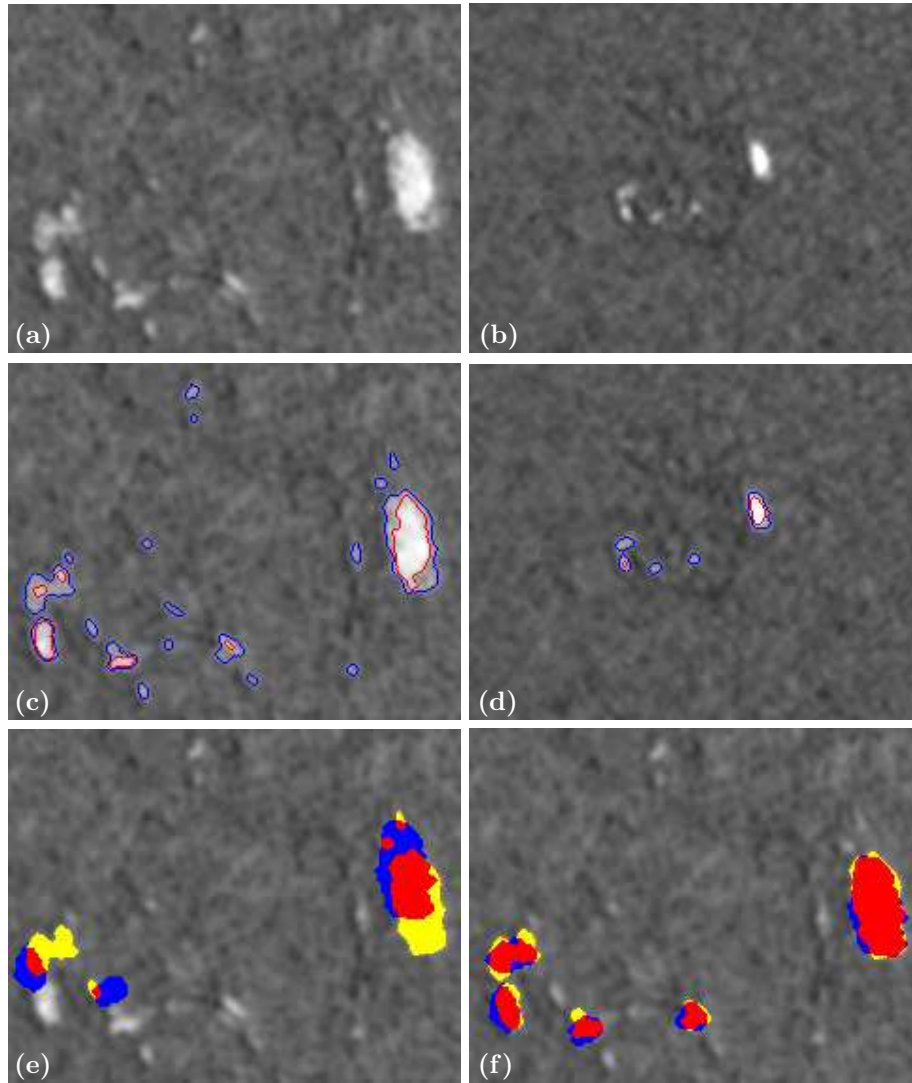
Figure 3. Identifying sunspots in SDO/HMI and SOHO/MDI images taken on 1 January 2011 at 00:13:10.20 and at 00:14:32 UT, respectively. (a) a sunspot group at the SE part of the SDO/HMI image. (b) the same group in the SOHO/MDI image. (c) and (d) the border contours of the sunspots: blue and red lines represet the penumbra and umbra borders of the spots, respectively. (e) HMI and MDI sunspot pixel sets and their correlation. MDI spot pixels are mapped onto the HMI solar disk using the MDI and HMI disk parameters: red pixels are the common pixels (intersection of the MDI and HMI spots), blue pixels belong only to MDI spots and yellow pixels belong only to HMI spots. Note that only the spots that have common pixels with the spots of the other image are colored. (f) the same as the (e) panel but the MDI image is mapped onto the HMI with the corrected MDI disk parameters.

One possible way to do this is by using their heliographic coordinates (the barycenter of the sunspots). But in the case of SDO and SOHO images this method is not too reliable owing to the large difference in their resolution, and, as we will see, to the errors in the solar disk parameters, and thus in heliographic coordinates. For this reason we choose a more reliable method. The algorithm of the method is as follows:

- The border contour pixels of the spots of the lower resolution image are mapped onto the higher resolution image. To this end, we need four parameters of both images separately: the solar disk radius, the row and column positions of the disk center, and the angle between the columns of CCD chip and the heliographic north direction of the solar disk (the disk parameters for short).
- The gaps between the adjacent transformed pixels of a contour are patched with line segments. There will be gaps because the lower resolution image is transformed into the higher one.
- The pixels of the spots (pixels inside the border contour, including the border contour itself) are determined both for the spots of the higher resolution image and for the spots mapped onto it.
- Now, a spot is considered as a pixel set. If the inequalities $\mid A \cap B \mid > \mid A \setminus B \mid$ and $\mid A \cap B \mid > \mid B \setminus A \mid$, for a transformed spot A and for a spot B of the higher resolution image, are true at the same time, and neither A nor B has intersection with other spots, then spots A and B are considered to be the same. Note that the above criteria tolerate some displacements and size differences between the corresponding spots.

Figure 3 exemplifies the process described before. If you examine Figure 3e systematically you can observe that, according to the above criteria, none of the five spots of the MDI image is identified with any spot of the HMI image. The cause is the large shift between the two images. If we investigate the full image, from which the partial image was cut out, we can observe that the amplitude and the direction of the shift of the spots depend on the heliographic coordinates of the spots. Therefore this shift is caused by the inaccuracy in the disk parameters of one of the images (or in both)

Following the steps given below, the disk parameters of one of the images can be adjusted to the other image (we adjust the MDI image to the HMI image).

- A function, whose maximum is sought, is constructed. It returns the number of the common pixels of the spots in HMI and the mapped MDI spots (i.e., total number of the pixels in the intersecting parts of the spots) as a function of the MDI solar disk parameters.
- Maximizing this function with respect to the MDI disk parameters results in the sought MDI disk parameters.

Figure 3f shows that, by using the new disk parameters obtained by the above process for the MDI image, all the five MDI sunspots are identified with corresponding HMI spots. The differences (new - original) for the disk parameters are the following: $\Delta R_\odot = -0.61$ pixels, $\Delta C_r = -0.51$ pixels, $\Delta C_c = -0.68$ pixels,

and $\Delta P = -0.26°$. Where $\Delta R_\odot$ is the solar disk radius difference, ΔC_r is the row index difference in the center of the solar disk, ΔC_c is the column index difference in the center of the solar disk, and ΔP is the difference in the solar pole direction. Note that the pixel values in the above quantities mean MDI image pixels (whose pixel array is 1024 x 1024).

There are fluctuations in these parameters from image to image. Their average values and standard deviations are: $\Delta R_\odot = -0.33 \pm 0.13$ pixels, $\Delta C_r = -0.22 \pm 0.13$ pixels, $\Delta C_c = -0.39 \pm 0.17$ pixels, and $\Delta P = -0.22 \pm 0.03°$. The 131 image pairs used to derive the above values were roughly uniformly chosen from 2200 pairs. An image pair was chosen so that they contained several sunspot groups well distributed over the solar disk. The most significant difference is of ΔP. This means that the north directions of the SOHO/MDI and the SDO/HMI images differ by 0.22°. To decide which of the two is the more accurate is outside the scope of this paper.

Finally, a short note is added to the possible cause of the inaccuracy of the disk parameters ($R_\odot$, C_r, and C_c). It is known that the MDI images have a slight ellipticity (Kuhn et al., 1998; Turmon et al., 2002). The difference between the major and the minor axes of the ellipse is $1''$. SAM also finds and corrects for it. But if this ellipticity is the consequence of CCD tilt (the optical axis is not perpendicular to the CCD chip), then a simple stretching or a squeezing of the solar disk along the proper direction is not the right way for the correction. The method discussed above can be tailored (supposing that the shift is caused by the CCD tilt) to determine the parameters that specify the CCD tilt, which can then be corrected.

5. SDO/HMI and SOHO/MDI Sunspot Area Comparison

In the subsections of this section, we perform the comparisons, for different solar features, between the areas obtained from HMI and MDI images.

5.1. Total Sunspot Area Comparison

Figure 4a depicts the scatterplot of the HMI total projected sunspot area ($A_{\mathrm{HMI}}^{\mathrm{tps}}$) versus the MDI total projected sunspot area ($A_{\mathrm{MDI}}^{\mathrm{tps}}$) and the regression line fitted to the data. The equation, the Root Mean Square Residual (RMR) of the regression line, and the correlation coefficient (r) are:

$$A_{\mathrm{HMI}}^{\mathrm{tps}} = (2.895 \pm 0.739) + (0.912 \pm 0.001) A_{\mathrm{MDI}}^{\mathrm{tps}} \quad RMR = 27.208 \quad r = 0.999 \quad (1)$$

As we can see, the HMI total projected sunspot areas are about 9 % smaller than the MDI ones.

Similarly, for the total corrected sunspot areas ($A_{\mathrm{HMI}}^{\mathrm{tcs}}$ and $A_{\mathrm{MDI}}^{\mathrm{tcs}}$) we have:

$$A_{\mathrm{HMI}}^{\mathrm{tcs}} = (4.171 \pm 0.769) + (0.905 \pm 0.001) A_{\mathrm{MDI}}^{\mathrm{tcs}} \quad RMR = 28.070 \quad r = 0.997 \quad (2)$$

Figure 4b depicts $TRAD$ *vs.* transformed MDI total sunspot areas. We can observe that the data more or less randomly fluctuate around the zero line, the amplitude of the fluctuations decreases with increasing area.
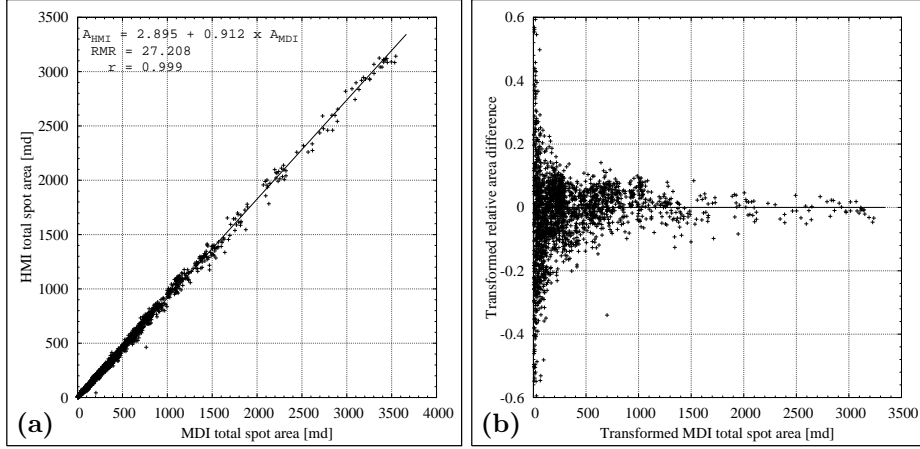
Figure 4. (a) HMI total projected sunspot area summed up on the whole disk *vs.* MDI total projected sunspot area (+) and a linear fit to the data (solid line). (b) *TRAD vs.* transformed MDI total projected spot area (+). The solid horizontal line through the origin represents the expectation value for identical HMI and transformed MDI areas.
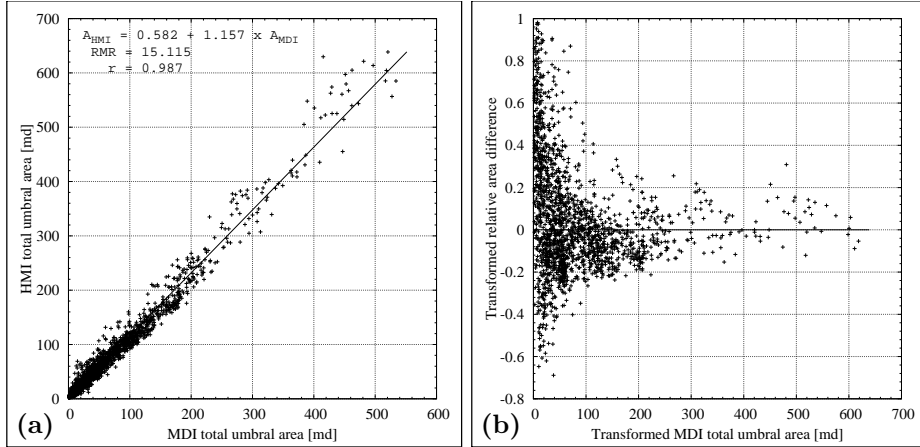

Figure 5. (a) HMI total projected umbral area summed up on the whole disk *vs.* MDI total projected umbral area (+) and a linear fit to the data (solid line). (b) *TRAD vs.* transformed MDI total projected umbral area (+). The solid horizontal line through the origin represents the expectation value for identical HMI and transformed MDI total projected umbral areas.

5.2. Total Umbra Area Comparison

Figure 5a depicts the scatterplot of the HMI total projected umbral area ($A_{\mathrm{HMI}}^{\mathrm{tpu}}$) versus the MDI total projected umbral area ($A_{\mathrm{MDI}}^{\mathrm{tpu}}$) and the regression line fitted to the data. The equation, the Root Mean Square Residual (RMR) of the regression line, and the correlation coefficient (r) are:

$$A_{\mathrm{HMI}}^{\mathrm{tpu}} = (0.582\pm0.455)+(1.157\pm0.004)A_{\mathrm{MDI}}^{\mathrm{tpu}} \quad RMR = 15.115 \quad r = 0.987 \quad (3)$$

As we can see, the HMI total projected umbral areas are about 16 % larger than the MDI ones.
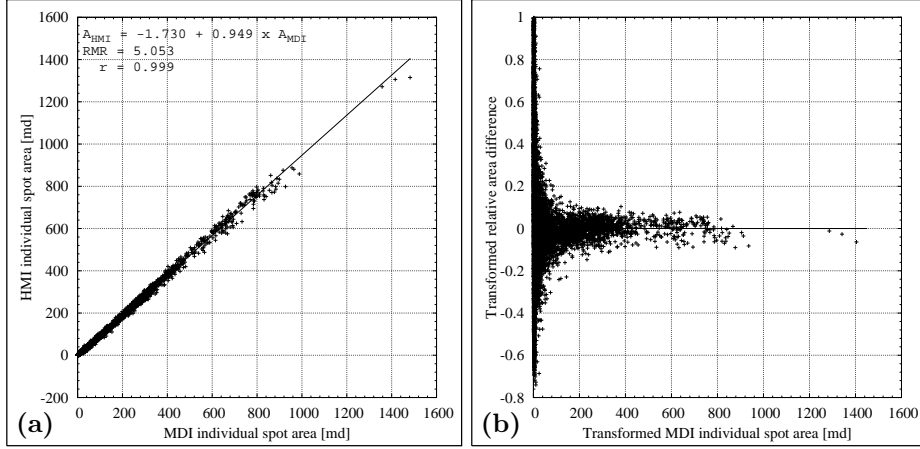
Figure 6. (a) HMI individual projected sunspot area summed up on the whole disk *vs.* MDI individual projected sunspot area (+) and a linear fit to the data (solid line). (b) $TRAD$ vs. transformed MDI individual projected sunspot area (+). The solid horizontal line through the origin represents the expectation value for identical HMI and transformed MDI individual projected sunspot areas.

Similarly, for the total corrected umbral areas ($A_{\mathrm{HMI}}^{\mathrm{tcu}}$ and $A_{\mathrm{MDI}}^{\mathrm{tcu}}$) we have:

$$A_{\mathrm{HMI}}^{\mathrm{tcu}} = (0.295 \pm 0.493) + (1.184 \pm 0.006) A_{\mathrm{MDI}}^{\mathrm{tcu}} \quad RMR = 15.868 \quad r = 0.974 \quad (4)$$

Figure 5b shows $TRAD$ *vs.* transformed MDI total projected umbral areas. We can observe some middle-term (relative to the data length) trends in the positions of the data around the zero line. The majority of the data between 100 and 200 md are bellow the zero line, and contrary to that the data between 440 and 600 md are above it. The amplitude of the fluctuations around the zero line decreases with increasing area.

5.3. Individual Sunspot Area Comparison

Figure 6a depicts the scatterplot of the HMI individual projected sunspot area ($A_{\mathrm{HMI}}^{\mathrm{ips}}$) versus the MDI total projected sunspot area ($A_{\mathrm{MDI}}^{\mathrm{tps}}$) and the regression line fitted to the data. The equation, the Root Mean Square Residual (RMR) of the regression line, and the correlation coefficient (r) are:

$$A_{\mathrm{HMI}}^{\mathrm{ips}} = (-1.730 \pm 0.048) + (0.949 \pm 0.000) A_{\mathrm{MDI}}^{\mathrm{ips}} \quad RMR = 5.053 \quad r = 0.999 \quad (5)$$

As we can see, the HMI individual projected sunspot areas are about 5 % smaller than the MDI ones.

Similarly, for the individual corrected sunspot areas ($A_{\mathrm{HIM}}^{\mathrm{ics}}$ and $A_{\mathrm{MIDI}}^{\mathrm{ics}}$) we have:

$$A_{\mathrm{HIM}}^{\mathrm{ics}} = (-0.901 \pm 0.065) + (0.937 \pm 0.001) A_{\mathrm{MIDI}}^{\mathrm{ics}} \quad RMR = 6.425 \quad r = 0.997 \tag{6}$$

Figure 6b depicts $TRAD$ vs. transformed MIDI individual projected spot areas. We can observe that the data randomly fluctuate around the zero line, the amplitude of the fluctuations decreases withncreasing area.
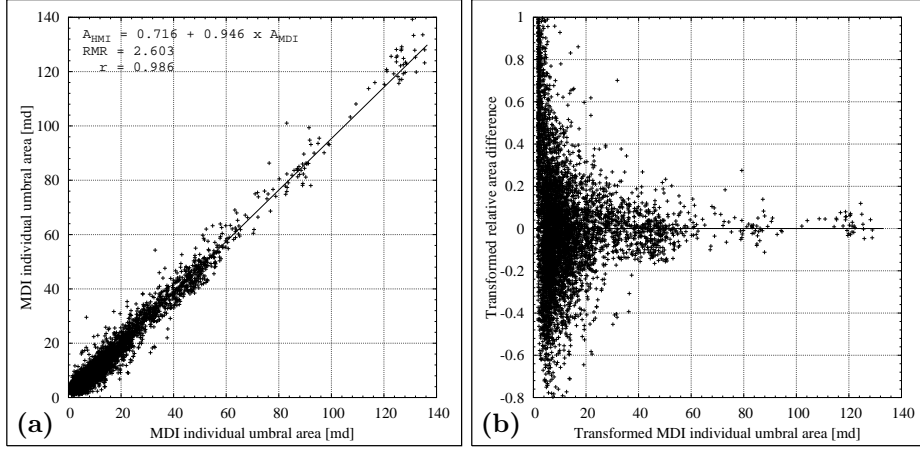
Figure 7. (a) HMI individual projected umbral area summed up on the whole disk *vs.* MDI individual projected umbral area (+) and a linear fit to the data (solid line). (b) *TRAD vs.* transformed MDI individual projected umbral area (+). The solid horizontal line through the origin represents the expectation value for identical HMI and transformed MDI individual projected umbral areas.

5.4. Individual Umbral Area Comparison

Figure 7a depicts the scatterplot of the HMI individual projected umbral area ($A_{\mathrm{HMI}}^{\mathrm{ipu}}$) versus the MDI individual projected umbral area ($A_{\mathrm{MDI}}^{\mathrm{ipu}}$) and the regression line fitted to the data. The equation, the Root Mean Square Residual (RMR) of the regression line, and the correlation coefficient (r) are:

$$A_{\mathrm{HMI}}^{\mathrm{ipu}} = (0.716 \pm 0.045) + (0.946 \pm 0.002)A_{\mathrm{MDI}}^{\mathrm{ipu}} \quad RMR = 2.603 \quad r = 0.986 \ (7)$$

As we can see, the HMI individual projected umbral areas are about 5 % smaller than the MDI ones.

Similarly, for the individual corrected umbral areas ($A_{\mathrm{HMI}}^{\mathrm{icu}}$ and $A_{\mathrm{MDI}}^{\mathrm{icu}}$) we have:

$$A_{\mathrm{HMI}}^{\mathrm{icu}} = (0.396 \pm 0.038) + (0.954 \pm 0.002)A_{\mathrm{MDI}}^{\mathrm{icu}} \quad RMR = 1.835 \quad r = 0.989 \ (8)$$

Figure 7b depicts *TRAD vs.* transformed MDI individual projected umbral areas. We can observe that the data randomly fluctuate around the zero line, the amplitude of the fluctuations decreases with increasing area.

6. Facular Area Comparison

Figure 8a depicts the scatterplot of the HMI total projected facular area ($A_{\mathrm{HMI}}^{\mathrm{tpf}}$) versus the MDI total projected facular area ($A_{\mathrm{MDI}}^{\mathrm{tpf}}$) and the regression line fitted to the data. The equation, the Root Mean Square Residual (RMR) of
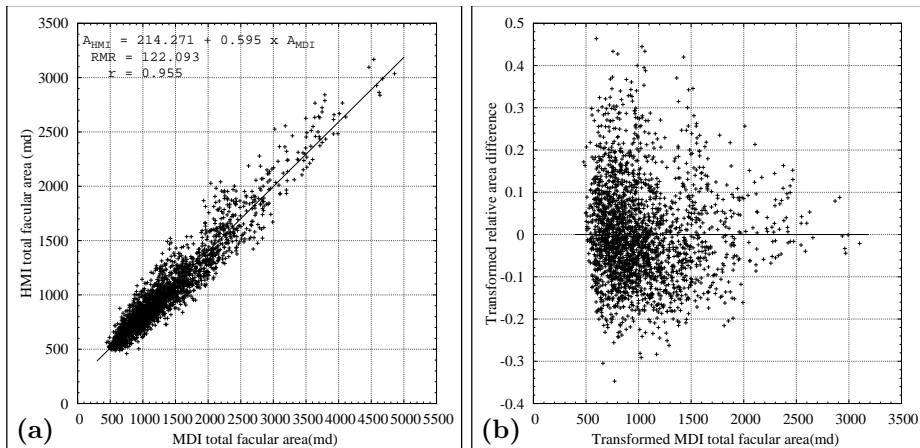
Figure 8. (a) HMI total projected facular area summed up on the whole disk *vs.* MDI total projected facular area (+) and a linear fit to the data (solid line). (b) *TRAD vs.* transformed MDI total projected facular area (+). The solid horizontal line through the origin represents the expectation value for identical HMI and transformed MDI total projected facular areas.

the regression line, and the correlation coefficient (r) are:

$$A_{\text{HMI}}^{\text{tpf}} = (214.271 \pm 5.811) + (0.595 \pm 0.004)A_{\text{MDI}}^{\text{tpf}} \quad RMR = 122.093 \quad r = 0.955 \tag{9}$$

As we can see, there is a very large difference between the data. The parameters of the linear regression are far from the ideal ones (zero for the y-intercep and 1 for the slope), see for explanation in Section 3.

Similarly, for the total corrected facular areas ($A_{\text{HMI}}^{\text{tcf}}$ and $A_{\text{MDI}}^{\text{tcf}}$) we have:

$$A_{\text{HMI}}^{\text{tcf}} = (260.408 \pm 8.746) + (0.674 \pm 0.005)A_{\text{MDI}}^{\text{tcf}} \quad RMR = 192.436 \quad r = 0.951 \tag{10}$$

Figure 8b depicts *TRAD vs.* transformed MDI projected facular areas. We can observe that the data randomly fluctuate around the zero line, the amplitude of the fluctuations decreases with increasing area.

7. Feature Number Comparison

Figure 9 illustrates the ratio of the numbers of different solar features in the HMI images to their numbers in the MDI images. As we can see HMI images have about two times more penumbrae (Figure 9a), about 2.5 times more umbrae (Figure 9b), and about three times more pores (Figure 9c) than MDI images.

The facula number ratio is even higher. HMI images have about five times more faculae than MDI, as it can be seen in Figure 9d (see for explanation in Section 3).
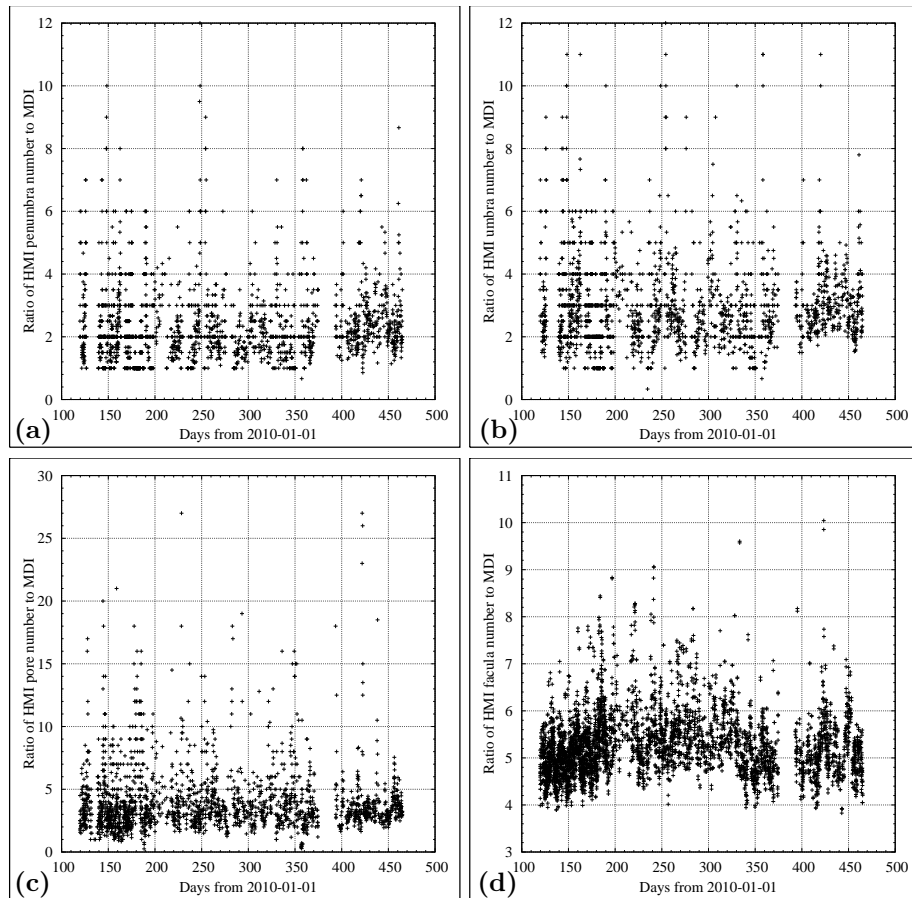
Figure 9. Comparison of the numbers of different solar features identified in HMI and MDI images. HMI to MDI ratio of the number of (a) penumbrae; (b) umbrae; (c) pores; (d) faculae.

8. Discussion and Conclusions

We have performed several types of comparison between the sunspot and facular areas, and between the feature numbers derived from the HMI and the MDI images. Moreover, we have given the equations that transform MDI- to HMI-measured areas. We did this to assist with the use of the feature areas derived from MDI and HMI images in diverse fields of solar physics.

The influence of the resolution on the measured areas of the solar features can be divided into two parts: systematic and random. The linear regression model is used to determine the systematic part. The $TRAD$ *vs.* transformed area plots characterize the random part. The basic causes of the random component are that a given value of the area of a feature can be realized with different feature structures, and that the measured area is the result of the interplay between the image resolution and the feature structure.

It is found that MDI individual areas (Figure 6, Equation (5), Figure 7, and Equation (7)) are closer to the HMI ones than total areas (Figure 4, Equation (1),

Figure 5, and Equation (3)). Individual areas are within 5 %, while for total areas the figures are: 9 % for total sunspot area and 16 % for total umbra area.

Generally, HMI areas are the smaller ones, except for the total umbral area. The MDI total umbral areas are 16 % smaller than the HMI ones, but, at the same time, the individual MDI umbral areas are 5 % larger. This means that the measured HMI umbral are not larger, but that more umbrae are found in the MDI images (see Figure 1 and Figure 9b).

By comparing the results for the total spot areas (MDI areas are 9 % larger) and for the individual spot areas (MDI areas are 5 % larger), they seem to contradict each other. Namely, we expect, on account of the result for the individual spot areas and of the fact that there are more spots in the HMI images than in the MDI ones (see Figure 1 and Figure 9c), that the total sunspot areas are closer to each other than the individual ones for the two datasets. We can resolve this contradiction by taking into account that the nearby spots merge in the MDI images yielding larger total areas by including the narrow regions separating them.

It is the measured facular area that is mostly influenced by the large resolution difference between the MDI and the HMI images (see for explanation in Section 3). It is also interesting to observe that the values of the total facular area are always above 450 md for the time interval of the data used for the comparison (see Figure 8).

We have also compared the number of solar features between the HMI and the MDI images. As expected, more features are found in the HMI images than in the MDI ones: about two times more penumbrae, about 2.5 times more umbrae, about three times more pores, and about five times more faculae. These numbers go much higher when large, complex sunspot groups are on the Sun (Figure 9).

As an interesting fact, we have found that there is a significant difference in the north direction between SOHO/MDI and SDO/HMI images. That, on average, amounts to the value of $0.22°$.

Acknowledgments

References

Baranyi, T., Győri, L., Ludmány, A., Coffey, H.E.: 2001, *Mon. Not. Roy. Astron. Soc.* **323**, 223.

Bovelet, B., Whier, E.: 2001, *Solar Phys.* **201**, 13.

Chapman, G. A., Dobias, J.J. Arias, T.: 2011, *Astrophys. J.* **728**, 150.

Domingo, V., Fleck, B., Poland, A.I.: 1995, *Solar Phys.* **162**, 1.

Fligge, M., Solanki, S.K.: 1997, *Solar Phys.* **173**, 427.

Fröhlich, C., Pap, J.M., Hudson, H.S.: 1994, *Solar Phys.* **152**, 111.

Győri, L.: 1998, *Solar Phys.* **180**, 109.

Győri, L., Baranyi, T., Turmon, M., & Pap, J.: 2004, *Adv. Space Res.* **34**, 269.

Győri, L.: 2005, *Hvar Obs. Bull.* **29**, 299.

Kuhn, J.R., Bush, R.I., Scheick, X., Scherrer, P.: 1998, *Nature* **392**, 155.

Oliver, R., Ballester, J.L.: 1994, *Solar Phys.* **152**, 481.

Pesnell, W.D., Thompson, B.J., Chamberlin, P.C.: 2012, *Solar Phys.* **275**, 3.

Turmon, M., Pap, J.M., Mukhtar, S.: 2002, *Astrophys. J.* **568**, 396.

Scherrer, P H., Bogart, R.S., Bush, R.I., Hoeksema, J.T., Kosovichev, A.G., Schou, J., Rosenberg, W., et al.: 1995, *Solar Phys.* **162**, 129.

Scherrer, P.H., Schou. J., Bush, R.I., Kosovichev, A.G, Bogart, R.S., Hoeksema, J.T., Liu, Y., et al.: 2012, *Solar Phys.* **275**, 207.

Wenzler, T., Solanki, S.K., Krivova, N.A., Fluri, D.M.: 2004, *Astron. Astrophys.* **427**, 1031